

Dinuclear Titanium(IV) Complexes from Amino Acid Bridged Dicatechol Ligands: Formation, Structure, and Conformational Analysis

Markus Albrecht,^{*,[a]} Matthias Napp,^[a] Matthias Schneider,^[a] Patrick Weis,^[b] and Roland Fröhlich^[c]

Abstract: Amino acid bridged dicatechol ligands **3a–e**-H₄ form dinuclear double-stranded coordination compounds [(**3a–e**)₂Ti₂(OCH₃)₂]²⁻ with titanium(IV) ions. Due to the directionality of the ligands, the chirality of the strand, and the chiral complex units, up to seven isomers, **I–VII**, can be obtained for the double-stranded complexes of ligands **3a–e**-H₄. The composition of the mixture of isomeric compounds in solution is strongly dependent on the conditions of complex formation. Under thermodynamic control, only a few isomers are obtained, one of which

is the major component of the mixture. X-ray structure analyses were performed for K₂[(**3b**)₂Ti₂(OH)₂] and K₂[(**3d**)₂Ti₂(OH)₂] (type **I**), and for the *meso*-complex Na₂[(**3e**)(**3e'**)Ti₂(OCH₃)₂]. A conformational analysis that uses Ramachandrans method revealed that the conformation of the amino acids in the ligand strands can be compared with those found for amino acids in helical

peptide structures. The most favored isomer of [(**3**)₂Ti₂(OCH₃)₂]²⁻ appears to be of type **I**, with the catecholamide unit located at the N terminus of the ligand strand that binds to a Δ -configured titanium(IV) complex unit and the dihydroxybenzyl group at the C terminus that coordinates to a Δ -configured titanium(IV) complex unit. The Δ configuration at the N terminus induces the conformation of a right-handed helix in the amino acid residue, while the Δ configuration induces the less favored left-handed helix.

Keywords: amino acids • conformational analysis • O ligands • self-assembly • titanium

Introduction

Very often, metalloproteins possess dinuclear complex units as the active center. The two metals are thus embedded in a peptic framework with additional small ligands (e.g. water or hydroxy) that bridge the metal ions. Such metalloproteins are for example hemerythrins, phosphatases, or ribonucleotide reductases. The separation of the two metal ions is typically in the range of 3 to 4 Å.^[1]

Artificial dinuclear complexes, in which the distance of the metal centers can be controlled, are double- or triple-stranded helicate-type coordination compounds.^[2–4] However, these are

not able to show enzyme-like activity, due to the lack of an available coordination site or the lack of a coligand that can be exchanged. Thus, ligands should be designed which, on the one hand, are able to fix two metal ions and, on the other hand, enable the binding of substrates.^[5]

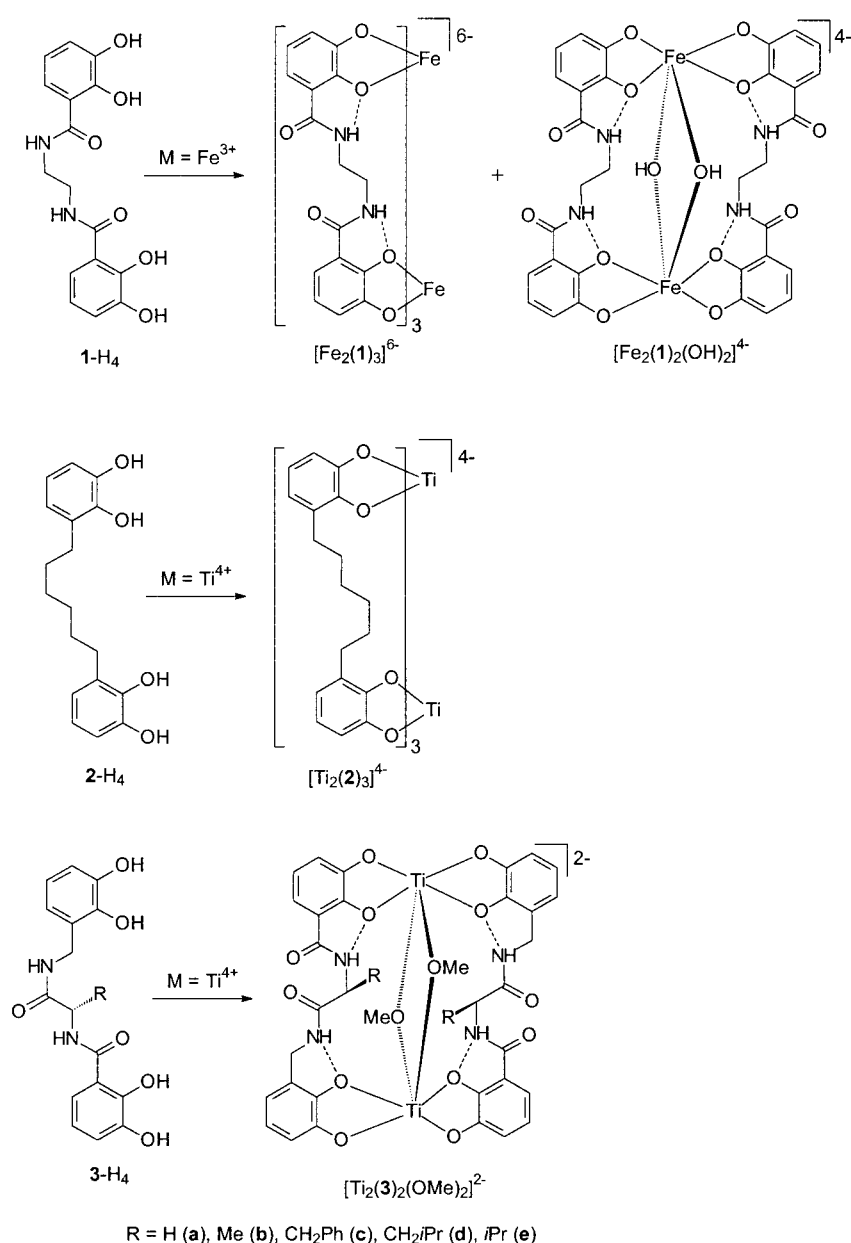
Our interest in the investigation of simple complexes that could act as a structural model for active centers in metalloproteins was initiated by the finding of Stack and Enemark that the dicatechol ligand **1**-H₄ is able to form either a triple-stranded dinuclear helicate [(**1**)₃Fe₂]⁶⁻ or a double-stranded dinuclear complex [(**1**)₂Fe₂(OH)₂]⁴⁻.^[6] In the latter, two hydroxy groups bridge the metal ions and should have the potential to be exchanged against other, more reactive coligands (Scheme 1). A close look at **1**-H₄ reveals that the spacer is composed of a chain of six atoms and it contains two amide linkages. Substitution of the spacer of **1**-H₄ by a pure (CH₂)₆-alkyl chain does not lead to the formation of a double-stranded complex. With **2**-H₄ and titanium(IV) ions, the triple-stranded helicate [(**2**)₃Ti₂]⁴⁻ was obtained exclusively.^[7] The two amide groups of **1**-H₄ seem to be essential for the formation of complexes such as [(**1**)₂Fe₂(OH)₂]⁴⁻.^[6]

Recently, the dicatechol ligands **3**-H₄, which bear an amino acid residue in the spacer, were introduced. The amino acid is linked by one amide unit to a catechol and by a second unit to a 2,3-dihydroxybenzyl group.^[8] Similar dicatechol

[a] Priv.-Doz. Dr. M. Albrecht, M. Napp, Dr. M. Schneider
Institut für Organische Chemie der Universität
Richard-Willstätter-Allee
76131 Karlsruhe (Germany)
Fax: (+49) 721-698529
E-mail: albrecht@ochhades.chemie.uni-karlsruhe.de

[b] Dr. P. Weis
Institut für Physikalische Chemie der Universität
Fritz-Haber-Weg
76128 Karlsruhe (Germany)

[c] Dr. R. Fröhlich
Organisch-chemisches Institut der Universität
Corrensstrasse 40
48149 Münster (Germany)



Scheme 1. Synthesis of the complexes.

ligands were used for the formation of triple-stranded helicates.^[4, 9, 10]

Previously, we reported that the phenylalanine-bridged derivative **3c-H₄** reacts with titanium(IV) ions in methanol to form a double-stranded complex [(**3c**)₂Ti₂(OCH₃)₂]²⁻. By negative ESI-MS, it could be shown that triple-stranded helicates are present only as minor traces. The composition of the obtained mixtures of diastereoisomers and regioisomers depends on kinetic or thermodynamic control of the reaction conditions. The X-ray structure of one isomer of [(**3c**)₂Ti₂(OCH₃)₂]²⁻ was described previously.^[11]

We present herein the coordination chemistry of ligands **3a–e-H₄** with titanium(IV) ions. The formation and characterization of the dinuclear complexes [(**3**)₂Ti₂(OR)₂]²⁻ is described. A conformational analysis of the amino acid residues of the solid-state structures of [(**3b**)₂Ti₂(OH)₂]²⁻, [(**3c**)₂Ti₂(OCH₃)₂]²⁻, [(**3d**)₂Ti₂(OH)₂]²⁻, and [(**3e**)₂Ti₂(OCH₃)₂]²⁻ allows us to draw conclusions about the preference of some regio- and stereoisomeric coordination compounds, and on the transfer of chiral information between peptide-like ligand strands and complex units.^[9, 12, 13]

Results and Discussion

The amino acid bridged ligands **3a–e-H₄** were prepared from 2,3-dimethoxybenzoic acid, L-amino acid, and 2,3-dimethoxy benzylamine as described earlier.^[14]

Two different procedures were used for the formation of complexes M₂[(**3**)₂Ti₂(OCH₃)₂] (M = alkali metal): 1) *Kinetic control of the reaction conditions*: Ligand **3-H₄**, [TiO(acac)₂] (1 equivalent each; acac = acetylacetonate) and alkali metal carbonate (0.5 equivalent) are dissolved in degassed methanol and stirred under argon for 16 h. The solvent was evaporated. If necessary, side products were removed by filtration of a methanol solution over Sephadex-LH20; 2) *Thermodynamic control of the reaction conditions*: The same protocol as for kinetic control is used, but the mixture is heated for 16 h under argon.

Complexes M₂[(**3**)₂Ti₂(OCH₃)₂] (M = Li, Na, K) are formed as red solids. For the compounds that contain alanine in the spacer M₂[(**3b**)₂Ti₂(OCH₃)₂], no correct elemental analysis was obtained. However, the complex could be characterized by ESI-MS and an X-ray structural analysis of one isomer was obtained.

Negative ESI mass spectrometric investigations: The ESI-MS spectrometric results for [(**3c**)₂Ti₂(OCH₃)₂]²⁻ were published previously.^[11] For the alanine derivative, signals of the double-stranded complex [(**3b**)₂Ti₂(OCH₃)₂]²⁻ are observed at *m/z* 865 (Na[(**3b**)₂Ti₂(OCH₃)₂]⁻) and 422 ([(**3b**)₂Ti₂(OCH₃)₂]²⁻).

Figure 1 shows representative examples of the negative ESI-MS spectra of the glycine- (Li₂[(**3a**)₂Ti₂(OCH₃)₂], (Figure 1 a)), alanine- (Li₂[(**3b**)₂Ti₂(OCH₃)₂], (Figure 1 b)), leucine- (Li₂[(**3d**)₂Ti₂(OCH₃)₂], (Figure 1 c)), and valine-bridged complexes (Li₂[(**3e**)₂Ti₂(OCH₃)₂], (Figure 1 d)) in methanol.

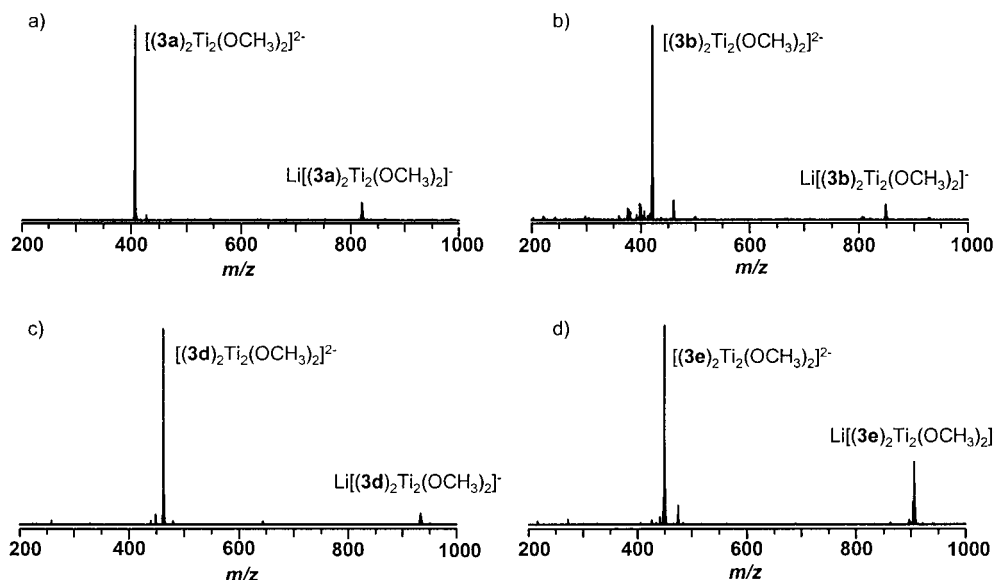


Figure 1. Negative-ion ESI-MS (methanol) spectra of $\text{Li}_2[(\mathbf{3a})_2\text{Ti}_2(\text{OCH}_3)_2]^{2-}$ (a), $\text{Li}_2[(\mathbf{3b})_2\text{Ti}_2(\text{OCH}_3)_2]^{2-}$ (b), $\text{Li}_2[(\mathbf{3d})_2\text{Ti}_2(\text{OCH}_3)_2]^{2-}$ (c) and $\text{Li}_2[(\mathbf{3e})_2\text{Ti}_2(\text{OCH}_3)_2]^{2-}$ (d).

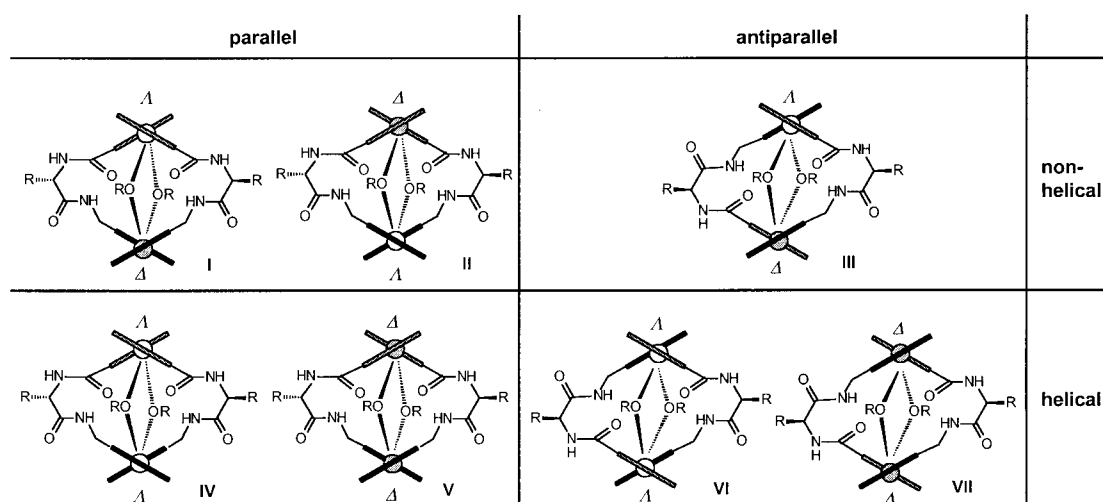


Figure 2. Schematic representation of the seven possible isomers of dinuclear double-stranded complexes $[(\mathbf{3a-e})_2\text{Ti}_2(\text{OCH}_3)_2]^{2-}$. The relative orientation of the directional ligands and the stereochemistry at the complex units are indicated. **I–III** possess a non-helical and **IV–VII** possess a helical arrangement of the ligands.

For all four complexes, two dominating peaks are detected, which correspond to the dianion $[(\mathbf{3})_2\text{Ti}_2(\text{OCH}_3)_2]^{2-}$ (m/z 407 (**a**), 421 (**b**), 463 (**d**), 449 (**e**)) and the monoanion $\text{Li}[(\mathbf{3})_2\text{Ti}_2(\text{OCH}_3)_2]^{-}$ (m/z 821 (**a**), 849 (**b**), 934 (**d**), 906 (**e**)).

The observed isotopic pattern of the peaks is in accordance with those obtained by calculation.

NMR spectroscopic investigations: Derivatives **3a–e-H₄** are directional ligands,^[15] for which one of the metal binding sites is attached to the N terminus of the amino acid and the other is attached to the C terminus. Thus, in a double-stranded dinuclear complex $[(\mathbf{3})_2\text{Ti}_2(\text{OCH}_3)_2]^{2-}$, the ligands can adopt a parallel or an anti-parallel orientation. Furthermore, due to the chirality at the metal complex units, seven isomers **I–VII** can be expected: three non-helical (**I–III**) and four helical (**IV–VII**) (Figure 2).^[16]

In case of the achiral glycine-bridged derivatives $[(\mathbf{3a})_2\text{Ti}_2(\text{OCH}_3)_2]^{2-}$, the isomers **I/II**, **IV/V**, and **VI/VII** are enantiomeric pairs. Thus, up to four sets of signals are expected for the NMR spectrum of $\text{Li}_2[(\mathbf{3a})_2\text{Ti}_2(\text{OCH}_3)_2]$. However, due to an overlap of the signals, the proton NMR spectrum cannot be unambiguously interpreted. On the other hand, the ¹³C NMR of $\text{Li}_2[(\mathbf{3a})_2\text{Ti}_2(\text{OCH}_3)_2]$ shows only two sets of major isomers in a 1:1 ratio. According to earlier observations,^[11] these two isomers are expected to be the non-helical (**I/II** and **III**) isomers. Model considerations on a semiempirical level (Spartan Plus, PM3) indicate that, in the helical isomers (**I–IV**), two of the four hydrogen bonds between amides and internal catechol-oxygen atoms have to be broken. In the non-helical isomers (**I–III**), four strong hydrogen bonds can be formed, which lead to an enhanced stability and a thermodynamic preference of the non-helical isomer compared with the helical isomers.^[11]

Substituents at the ligands with chiral amino acids in the spacer **3b–e**-H₄ lead to dinuclear complexes [(**3b–e**)₂Ti₂(OCH₃)₂]²⁻, in which isomers **I/II**, **IV/V**, and **VI/VII** are diastereomeric pairs. Isomers **I**, **II**, and **IV–VII** possess a C₂ symmetry axis. Non-helical isomer **III** is unsymmetric. Therefore up to eight sets of signals are expected for the mixture of isomeric complexes [(**3b–e**)₂Ti₂(OCH₃)₂]²⁻.

In the case of the phenylalanine-derived complex [(**3c**)₂Ti₂(OCH₃)₂]²⁻, we were able to observe all seven of the possible isomers with the use of a benzylic CH₂N proton of the ligand as an NMR probe.^[11] For the L-alanine derivative [(**3b**)₂Ti₂(OCH₃)₂]²⁻, ¹H and ¹³C NMR spectra were obtained in [D₄]methanol, but could not be interpreted.

Only four isomers were detected for [(**3d**)₂Ti₂(OCH₃)₂]²⁻ and [(**3e**)₂Ti₂(OCH₃)₂]²⁻. However, the NMR spectra of the complexes obtained under kinetic control were very complicated, while the spectra (especially the ¹³C NMR spectrum) of the mixtures formed under thermodynamic control were very informative. Only three species, one of which dominates, were present.

In Figure 3, the change of the isomer ratio is shown with the help of a diagnostic aromatic resonance (dd) of [(**3d**)₂Ti₂(OCH₃)₂]²⁻ as a representative example. After 13 days, only one major and one minor species were detected, along with traces of two other isomers. The observation of only one double doublet for the proton of each of the isomers excludes the presence of unsymmetric isomer (**III**) in the “final” mixture.

X-ray structures of K₂[(**3b**)₂Ti₂(OH)₂]·5DMF·3H₂O, K₂[(**3d**)₂Ti₂(OH)₂]·6DMF, and Na₂[(**3e**)(**3e'**)Ti₂(OCH₃)₂]·6DMF·diethyl ether:

The X-ray structure of Li₂[(**3c**)₂Ti₂(OCH₃)₂]·4DMF·2H₂O was reported earlier.^[11] In the solid state, structure **III**, with opposite orientation of ligands **3c**, is observed for dianion [(**3c**)₂Ti₂(OCH₃)₂]²⁻ (Figure 4).

K₂[(3b**)₂Ti₂(OH)₂]·5DMF·3H₂O:** The alanine-bridged complex K₂[(**3b**)₂Ti₂(OH)₂] crystallizes in the orthorhombic space group P2₁2₁2₁. Because the crystals of K₂[(**3b**)₂Ti₂(OH)₂] were of poor quality, only a poor X-ray structure (R = 15.9) was obtained. Two μ-hydroxy groups and two titanium(IV) ions form a dimeric central four-membered [Ti(μ-OH)₂]₂ ring.^[17] The two ligands **3b** bridge the two titanium(IV) centers and are orientated parallel to each other. The complex unit at the “N terminus” of the L-alanine-bridged ligands is Δ- and the unit at the “C terminus” is Λ-configured. Thus, the “side-by-side”^[3, 18] isomer **I** is observed (Figure 4).

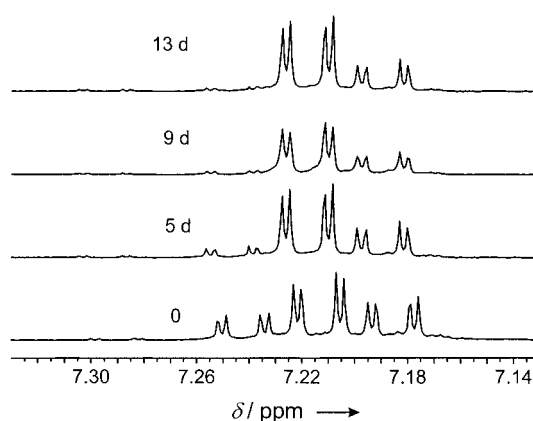


Figure 3. Part of the ¹H NMR spectrum ([D₄]methanol) of the complex [(**3d**)₂Ti₂(OCH₃)₂]²⁻ that shows the presence of four different isomers in the mixture which was produced under kinetically controlled reaction conditions. Within 13 days, it is transformed into the “thermodynamic” product mixture.

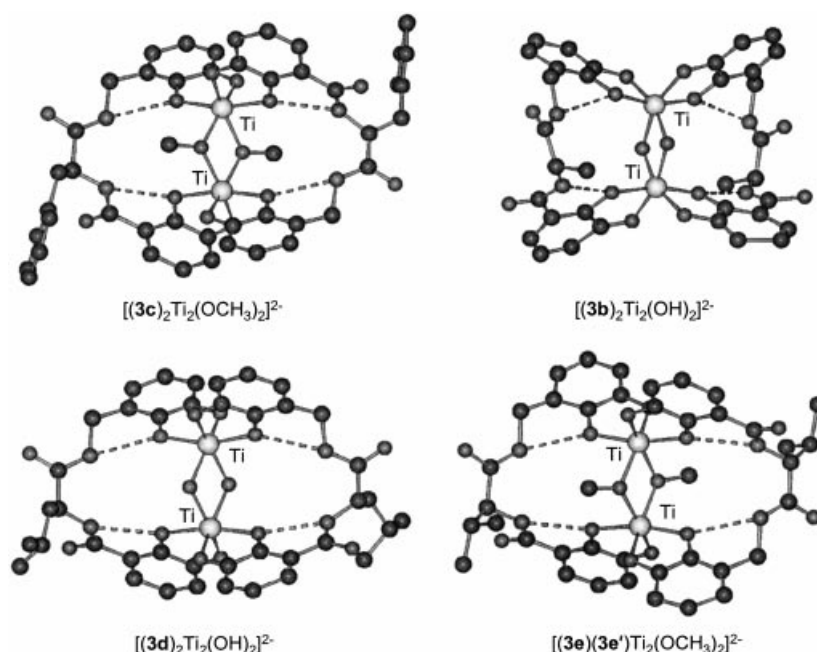


Figure 4. Solid-state structure of dianions [(**3c**)₂Ti₂(OCH₃)₂]²⁻,^[11] [(**3b**)₂Ti₂(OH)₂]²⁻, [(**3d**)₂Ti₂(OH)₂]²⁻, and [(**3e**)(**3e'**)Ti₂(OCH₃)₂]²⁻.

K₂[(3d**)₂Ti₂(OH)₂]·6DMF:** The leucine-bridged derivative K₂[(**3d**)₂Ti₂(OH)₂]·6DMF crystallizes in the orthorhombic space group P2₁2₁2₁ and was refined to R = 0.076. For the dianion of the leucine derivative [(**3d**)₂Ti₂(OH)₂]²⁻ (Figure 4), a related structure to the alanine-bridged complex [(**3b**)₂Ti₂(OH)₂]²⁻ is observed. The two ligands **3d** are orientated parallel with one Δ-configured complex unit at the “N terminus” and one Λ-configured at the “C terminus” of the strand. The two metal centers are bridged by two ligands **3d** and additionally by two hydroxy groups, which form a central four-membered [Ti(μ-OH)₂]₂ ring. Angles in this ring are Ti–O–Ti 106.3°/105.7° and O–Ti–O 73.9°/74.1° with Ti–O distances of 1.978 to 2.000 Å. The separation of the two metal centers is 3.175 Å. Both potassium cations of K₂[(**3d**)₂Ti₂(OH)₂] are hexacoordinate with a pseudooctahedral coordination geometry. Each of them is bound to the Δ-configured

titanium complex moiety, which interacts with the terminal catecholate oxygen atom of one ligand strand (K–O 2.711/2.759 Å) and with the internal catechol oxygen of the second strand (K–O 2.855/2.912 Å). Further, three DMF molecules coordinate to each K⁺ ion (K–O 2.610–2.829 Å). A further coordination site is filled by an amide oxygen atom at the “C terminus” of a neighboring complex unit (K–O 2.647/2.630 Å). Thus, an infinite polymeric chain is formed in the solid state (Figure 5).^[19]

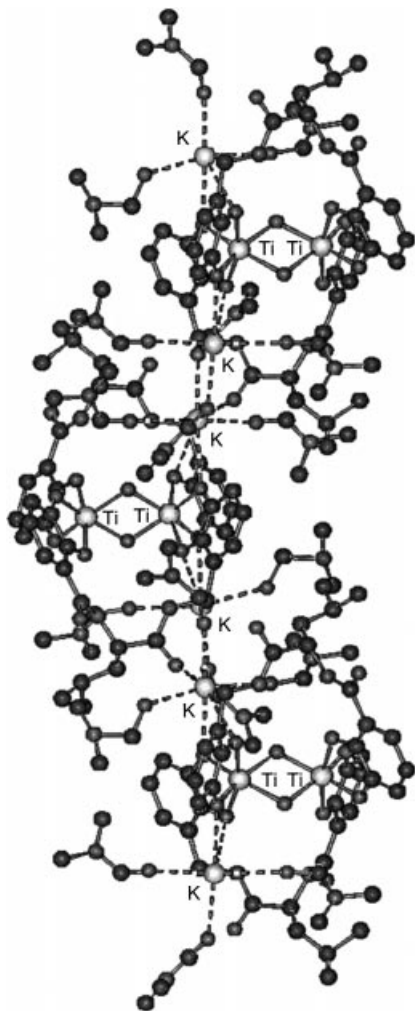


Figure 5. The polymeric structure of $K_2[(3d)_2Ti_2(OH)_2] \cdot 6DMF$ in the solid state.

$Na_2[(3e)(3e')Ti_2(OCH_3)_2] \cdot 6DMF \cdot diethyl\ ether$: Only one crystal of the valine-bridged complex which was suitable for X-ray investigations was obtained. To our surprise, we did not have the expected chiral complex $Na_2[(3e)_2Ti_2(OCH_3)_2]$, but the *meso* form $Na_2[(3e)(3e')Ti_2(OCH_3)_2]$, which contains one strand with the D-(3e') and one with the L-amino acid (3e). We believe that only traces of this complex were formed, because of minor amounts of racemization during the synthesis of $3e-H_4$.^[20]

The *meso* complex $Na_2[(3e)(3e')Ti_2(OCH_3)_2]$ crystallizes in the triclinic space group $P\bar{1}$ with a center of inversion in the

molecule, which makes the two complex units and the ligand strands equivalent by symmetry.

Dianion $[(3e)(3e')Ti_2(OCH_3)_2]^{2-}$ adopts a structure in which the two metal centers are configured oppositely. The “N terminus” of the *S*-configured ligand **3e** binds to the complex unit which is *A*-configured. The “unnatural” *R*-configured ligand **3e'** is orientated in the opposite direction. Each of the two oppositely configured ligands **3e** and **3e'** binds to both titanium(IV) centers, which are additionally bridged by two methoxy groups that form a central four-membered (Ti–O–Ti–O) ring (angles: Ti–O–Ti 106.13°, O–Ti–O 73.87°; distances: Ti–O 1.995, 2.000 Å, Ti–Ti 3.193 Å).^[17]

The two sodium cations are also equivalent by symmetry. They possess a geometry that is close to a trigonal-bipyramidal coordination geometry, binding to three DMF molecules (Na–O 2.230–2.405 Å) and to two of the amide oxygen atoms at the N terminus of the amino acid residues (Na–O 2.267–2.400 Å).

Conformational considerations: To understand the preferred formation of some of the isomers **I–VII** under thermodynamic control of the reaction, we have to consider the conformational features of ligands **3a–e** that bridge the metal centers of the complexes $[(3a–e)_2Ti_2(OR)_2]^{2-}$. Figure 6a shows three parts *a–c* of ligands **3a–e** that have different influences on the formation and structure of the dinuclear double-stranded complexes $[(3a–e)_2Ti_2(OR)_2]^{2-}$:

a) 2,3-Dihydroxybenzoic acid is attached to the N terminus of the central amino acid. When metal coordination occurs, an intramolecular hydrogen bond is formed between the amide NH and the internal catechol oxygen atom. This leads to a very rigid, nearly planar catecholamide unit.^[13, 21] A measure for the deviation from planarity in the resulting hydrogen-bridged six-membered ring is the dihedral angle Ω (N–C(O)–C(1)_{ipso}–C(2)); Figure 6a, Table 1). In the X-ray structures of complexes $[(3c–e)_2Ti_2(OR)_2]^{2-}$, dihedral angles of $\Omega = -8.95$ – 8.95° were found. Only the alanine-derived ligands **3b** had somewhat larger angles of $\Omega = -15.53$ and -19.69° in complex $[(3b)_2Ti_2(OH)_2]^{2-}$. This shows that the catecholamide units are nearly planar, with only slight deviations from planarity.

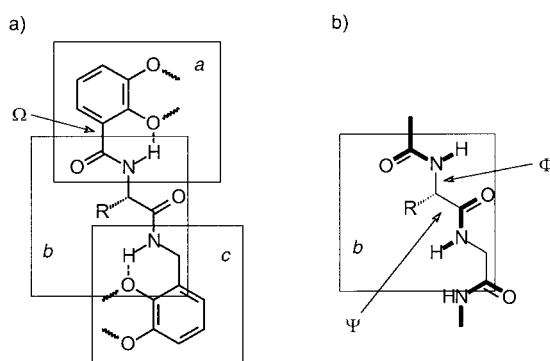


Figure 6. a) Presentation of amino acid bridged ligands **3a–e** in the dinuclear complexes $[(3)_2Ti_2(OR)_2]^{2-}$, showing the rigid catecholamide unit *a*, the peptide-like spacer *b*, and the flexible benzylamide moiety *c*. b) A small peptide chain which shows the analogy to the spacer of **3a–e**. Ω , Φ , and Ψ define dihedral angles at the bonds marked by an arrow.

Table 1. Dihedral angles Φ , Ψ , and Ω observed for the ligands **3b–e** in the solid-state structures of the complexes $[(\mathbf{3b-e})_2\text{Ti}_2(\text{OR})_2]^{2-}$.

	Φ [°]	Ψ [°]	Ω [°]
3b -(1)	−80.66	−22.5	−15.53
3b -(2)	−85.29	−17.77	−19.69
3c -(1)	80.53	30.69	6.00
3c -(2)	−115.11	5.8	−3.13
3d -(1)	−90.51	−25.22	−0.70
3d -(2)	−88.84	−20.97	−6.39
(<i>S</i>)- 3e	−115.46	13.37	−8.95
(<i>R</i>)- 3e'	115.46	−13.37	8.95

b) The spacer of ligands **3a–e** possesses some structural relevance to a “dipeptide” unit (Figure 6b). Rigid, planar parts are shown in bold lines, more flexible parts are presented as thin lines. At the N terminus of the central amino acid (glycine, alanine, phenylalanine, leucine or valine), the rigid and planar catecholamide unit *a* is attached. The conformation of the amino acid can be described by Ramachandran’s method with the use of the dihedral angles Φ and Ψ .^[22–24] At the C terminus of the amino acid, 2,3-dihydroxybenzyl amine *c* is attached by an amide linkage.

c) Part *c* of the ligand can be compared with a glycine residue, substituting the sp^2 -carbon atom of the C terminus by the *ipso*-carbon atom of the catecholate moiety. The NH group of the 2,3-dihydroxybenzyl amide of **3b–e** is able to undergo intramolecular hydrogen bonding interactions with the internal catecholate oxygen atom of the benzyl group. Owing to the conformational flexibility at the CH_2 unit, this hydrogen bonding is not as strong as was observed for catecholamide moiety *a*.^[21] Significant deviation from planarity is found for the hydrogen-bridged six-membered ring.

The angles Φ and Ψ , which are found in the X-ray structures of $[(\mathbf{3b-e})_2\text{Ti}_2(\text{OR})_2]^{2-}$, are listed in Table 1, and the corresponding Ramachandran plot^[22–24] is shown in Figure 7.

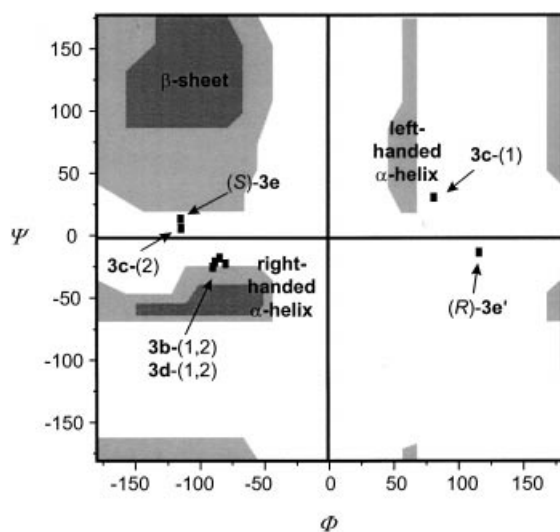


Figure 7. Ramachandran plot for the dihedral angles Φ/Ψ of the central amino acid residues of **3b–e**. The angles were obtained from the results of the X-ray structural analyses. The dark gray regions represent highly favored and the gray regions favored conformations of the amino acids.

For the alanine- and leucine-bridged complexes $[(\mathbf{3b})_2\text{Ti}_2(\text{OH})_2]^{2-}$ and $[(\mathbf{3d})_2\text{Ti}_2(\text{OH})_2]^{2-}$, the dihedral angles at the central amino acid (Φ/Ψ) are found in a region of the Ramachandran plot in which amino acid residues of peptides with a right-handed helical conformation are usually observed.^[23, 24]

In the case of phenylalanine derivative $[(\mathbf{3c})_2\text{Ti}_2(\text{OCH}_3)_2]^{2-}$, the two ligands **3c** are orientated differently and adopt different conformations. The conformation of the phenylalanine of the one ligand strand, **3c**-(2), which is bound through its catecholamide unit to the Δ -configured titanium center, is between the regions of Φ/Ψ values that are typically found for right-handed helices and for sheet-structures. The conformation might be best described as a twisted sheet with a right-handed conformation.^[23] The other ligand strand, **3c**-(1), coordinates with its catecholamide unit (N terminus) to the Δ -configured titanium center. Dihedral angles (Φ/Ψ) are observed in the region of a left-handed helical peptide.^[23]

Typical conformations of amino acid residues of twisted sheet-type peptide structures were found for the valine-moieties of $[(\mathbf{3e})(\mathbf{3e}')\text{Ti}_2(\text{OCH}_3)_2]^{2-}$. The *S*-configured ligand, (*S*)-**3e**, is attached through the catecholamide unit to the Δ -configured titanium center and adopts a right-handed conformation that is close to that observed for the phenylalanine derivative, **3c**-(2). Due to the inversion symmetry found in $[(\mathbf{3e})(\mathbf{3e}')\text{Ti}_2(\text{OCH}_3)_2]^{2-}$, both ligands adopt a similar conformation with opposite signs of the dihedral angles. (*R*)-**3e'** binds with its N terminal catecholamide unit to the Δ -configured titanium center and shows structural features of a twisted left-handed sheet.

The data of the Ramachandran plot in Figure 7 can be separated into two different sets: one with a right-handed helical conformation (**3b**-(1,2), **3c**-(2), **3d**-(1,2), and (*S*)-**3e**) and one with a left-handed helical conformation (**3c**-(1) and (*R*)-**3e'**) at the amino acid residue. The ligand strands with a right-handed twist bind through their N-terminal catechol moieties to Δ - and with their C terminus to Δ -configured complex units. For the ligands that possess a left-handed turn, the situation is opposite to that of ligands with right-handed turns.

Our perception is that the stereochemical communication between the ligand spacer and the metal complex units occurs through the very rigid N-terminal catecholamide unit. The C-terminal binding site is more flexible, due to the sp^3 -carbon atom in the six-membered hydrogen-bonded ring. The deviation from planarity of this unit in the X-ray structures shows that this moiety is able to level out constraints that are built up during complex formation.

What are the consequences of ligand strand conformations on the specific formation of only a few of the isomeric complexes **I–VII** $[(\mathbf{3a-e})_2\text{Ti}_2(\text{OR})_2]^{2-}$?

1) As discussed before, helical structures **IV–VII** should be disfavored compared with non-helical structures **I–III**, due to reduced stabilizing hydrogen bonding interactions.^[11] As expected, only X-ray structures of non-helical isomers were obtained.

2) Our conformational considerations with the use of Ramachandran’s method^[22] indicate that a Δ -configuration at the N-terminal complex unit induces a right-handed confor-

mation of the amino acid. Consequently, a left-handed twist is induced by a Δ configuration at the N terminus. However, the left-handed conformation is unfavorable for L-amino acid residues, due to the steric interaction with the peptide backbone.^[23]

This indicates that, in the favored isomer of the double-stranded complexes $[(\mathbf{3b-e})_2\text{Ti}_2(\text{OR})_2]^{2-}$, both ligand strands adopt a right-handed conformation. However, this is only possible if both ligand strands are orientated parallel and bind with their N-terminal catechol unit to a Δ -configured titanium complex unit. Therefore, nonhelical isomer **I**, as it was found in the X-ray structures of $[(\mathbf{3b})_2\text{Ti}_2(\text{OH})_2]^{2-}$ and $[(\mathbf{3d})_2\text{Ti}_2(\text{OH})_2]^{2-}$, should be the thermodynamically favored isomer. Consequently, isomer **III**, which was found in the X-ray structure of $[(\mathbf{3c})_2\text{Ti}_2(\text{OCH}_3)_2]^{2-}$, is not thermodynamically favored, as already shown by NMR spectroscopy.^[11]

For *meso* complex $[(\mathbf{3e})(\mathbf{3e}')\text{Ti}_2(\text{OCH}_3)_2]^{2-}$, the thermodynamically preferred isomer with antiparallel orientation of the ligands is observed in the solid state. Both amino acid residues possess the favored right-handed (*S*-**3e**) or left-handed (*R*-**3e'**) conformation.

Due to the lack of an α -substituent, there is no preference for the left- or right-handed conformation in the case of the glycine-bridged ligand **3a**. This does not lead to a thermodynamic preference of one of the possible non-helical regioisomers **I/II** or **III**, which gives an explanation for the observation of two dominating species (1:1 ratio) in the ¹³C NMR spectrum of $[(\mathbf{3a})_2\text{Ti}_2(\text{OCH}_3)_2]^{2-}$.

Conclusion

Directional dicatechol ligands **3a–e-H₄** that possess amino acid residues in the spacer form double-stranded dinuclear titanium(IV) complexes $\text{M}_2[(\mathbf{3a-e})_2\text{Ti}_2(\text{OR})_2]$ with additional coligands present. Due to the unique conformational features of the amino acids and due to the stereochemical information embedded in the ligands and the complex units, a specific formation of only a few of the possible stereo- and regioisomers is observed. Conformational considerations indicate a coupling of the chirality at the complex units with the conformation of the amino acid residues. The presented results thus indicate that nonhelical isomer **I**, with two ligand-strands orientated parallel and binding with their N-terminal binding site to a Δ -configured complex unit, is the thermodynamically favored species, when chiral ligands **3b–e-H₄** are used (Figure 8).

The titanium-bound coligands $\mu\text{-OR}^-$ are fixed in a pocket of amino acid residues and thus might act as a very simple artificial structural model for the binding of substrates in metalloenzymes. However, there is no functional similarity!

Experimental Section

General remarks: ¹H and ¹³C NMR spectra were recorded on a Bruker DRX 500 NMR spectrometer. FT-IR spectra were recorded on a Bruker IFS spectrometer. The UV/Vis spectra were measured with a Perkin Elmer Lambda 2 spectrometer. Negative-ion ESI MS spectra were taken on a Bruker Bioapex II FTMS equipped with a 7 Tesla magnet. Elemental

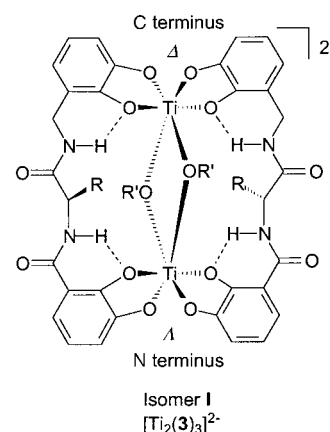


Figure 8. Thermodynamically favored isomer **I** of the double-stranded dinuclear complexes $[(\mathbf{3b-e})_2\text{Ti}_2(\text{OR})_2]^{2-}$.

analyses were obtained with a Heraeus CHN-O-Rapid analyzer. Ligands were prepared as described in reference [8]

Data sets were collected with a Nonius KappaCCD diffractometer, equipped with a rotating anode generator Nonius FR591. Programs used: data collection COLLECT (Nonius B.V., 1998), data reduction DENZO-SMN,^[25] absorption correction SORTAV,^[26] structure solution SHELXS-97,^[27] structure refinement SHELXL-97, (G.M. Sheldrick, Universität Göttingen, 1997) graphics SCHAKAL.^[28]

Crystallographic data (excluding structure factors) for the structures reported in this paper have been deposited with the Cambridge Crystallographic Data Center as supplementary publication nos. CCDC-149451, CCDC-160958, and CCDC-160959. Copies of the data can be obtained free of charge on application to CCDC, 12 Union Road, Cambridge CB21EZ, UK (fax: (+44) 1223-336-033; e-mail: deposit@ccdc.cam.ac.uk).

General procedures for the preparation of complexes $\text{M}_2[(\mathbf{3})_2\text{Ti}_2(\text{OCH}_3)_2]$ ($\text{M} = \text{Li, Na and/or K}$):

1) Kinetic control of the reaction conditions: In a typical experiment, ligand **3-H₄** (1 equiv, ca. 20–50 mg), $[\text{TiO}(\text{acac})_2]$ (1 equiv; acac = acetylacetonate) and M_2CO_3 (0.5 equiv) are dissolved in degassed methanol (30 mL) and are stirred under argon for 16 h. Solvent was evaporated and a red-orange solid remained. The crude product can be purified by filtration over Sephadex-LH20 (methanol). **2) Thermodynamic control of the reaction conditions:** A similar experiment is performed with heating of the mixture for 16 h under argon.

Li₂[(3a**)₂Ti₂(OCH₃)₂]:** ¹H NMR ($[\text{D}_4]$ methanol, 500 MHz): $\delta = 7.3\text{--}7.0$ (Σ 1 H), 6.6–6.2 (Σ 5 H), 4.71–4.65 (m, 1H), 4.61–4.45 (m, 1H), 4.18–4.01 (m, 1H), 3.82–3.72 (m, 1H); ¹³C NMR ($[\text{D}_4]$ methanol, 125.8 MHz, two dominating sets of signals): $\delta = 172.4$ (C), 172.1 (C), 169.4 (C), 169.1 (C), 161.1 (C), 160.8 (C), 160.7 (C), 160.3 (C, double intensity), 160.1 (C), 159.2 (C), 159.0 (C), 120.8 (CH), 120.6 (CH, two signals), 120.3 (CH), 119.8 (CH), 119.4 (CH), 119.1 (CH), 119.0 (C, double intensity), 118.8 (CH), 115.9 (C), 115.5 (C), 115.3 (CH), 114.9 (CH), 111.8 (CH), 111.6 (CH), 44.1 (CH₂), 43.8 (CH₂), 43.2 (CH₂), 43.1 (CH₂); negative-ion ESI MS (methanol): m/z 407 ($[(\mathbf{3a})_2\text{Ti}_2(\text{OCH}_3)_2]^{2-}$), 821 ($[\text{Li}[(\mathbf{3a})_2\text{Ti}_2(\text{OCH}_3)_2]^-]$); elemental analysis calcd (%) for $\text{C}_{34}\text{H}_{30}\text{Li}_2\text{N}_4\text{O}_{14}\text{Ti}_2 \cdot 14\text{H}_2\text{O}$: C 37.79, H 5.41, N 5.19; found: C 37.67, H 5.03, N 5.03.

Li₂[(3b**)₂Ti₂(OCH₃)₂]:** ¹H NMR ($[\text{D}_4]$ methanol, 500 MHz): $\delta = 7.19, 7.13\text{--}7.02$ (2 m, Σ 1H), 6.6–6.4 (m, 4H), 6.28–6.24 (m, 1H), 4.77 (m, 1H), 4.46 (m, 1H), 4.22–4.08 (m, 1H), 1.66–1.59 (m, 3H); ¹³C NMR ($[\text{D}_4]$ methanol, 125.8 MHz): $\delta = 175.9, 175.6, 175.3, 170.1, 169.8, 169.7, 168.8, 168.5, 162.2, 161.3, 161.0, 160.7, 160.6, 160.4, 160.2, 160.1, 160.0, 159.9, 159.8, 159.3, 159.2, 159.0, 120.8, 120.6, 120.4, 119.9, 119.4, 119.1, 118.8, 118.5, 118.3, 118.1, 118.0, 117.9, 117.7, 117.3, 115.9, 115.5, 115.3, 115.2, 115.1, 115.0, 114.9, 114.8, 114.6, 114.2, 111.8, 111.6, 111.4, 44.8, 44.5, 44.3, 44.0, 19.8, 19.3, 19.2, 19.0, 18.8, 18.3$; negative-ion ESI MS (methanol): m/z 421 ($[(\mathbf{3b})_2\text{Ti}_2(\text{OCH}_3)_2]^{2-}$), 849 ($[\text{Li}[(\mathbf{3b})_2\text{Ti}_2(\text{OCH}_3)_2]^-]$); $\text{Li}_2[(\mathbf{3b})_2\text{Ti}_2(\text{OCH}_3)_2]$ could not be obtained in analytically pure form.

Na₂[(3b**)₂Ti₂(OCH₃)₂]:** Negative-ion ESI MS (methanol): m/z 422 ($[(\mathbf{3b})_2\text{Ti}_2(\text{OCH}_3)_2]^{2-}$); 865 ($[\text{Na}[(\mathbf{3b})_2\text{Ti}_2(\text{OCH}_3)_2]^-]$); $\text{Na}_2[(\mathbf{3b})_2\text{Ti}_2(\text{OCH}_3)_2]$ could not be obtained in analytically pure form.

K₂[(3b)₂Ti(OCH₃)₂]: X-ray quality crystals were obtained by crystallization from wet DMF/diethyl ether. X-ray crystal structure analysis of K₂[(3b)₂Ti(OCH₃)₂]: formula C₃₄H₃₀N₄O₁₄K₂Ti₂·6 C₃H₇NO·2 H₂O, *M_r* = 1367.23, red crystal 0.15 × 0.10 × 0.05 mm, *a* = 13.364(1), *b* = 19.113(1), *c* = 25.204(1) Å, *V* = 6437.8(6) Å³, ρ_{calcd} = 1.411 g cm⁻³, μ = 4.58 cm⁻¹, no absorption correction (0.934 ≤ *T* ≤ 0.977), *Z* = 4, orthorhombic, space group *P*2₁2₁2₁ (no. 19), λ = 0.71073 Å, *T* = 198 K, ω and φ scans, 8179 reflections collected (±*h*, ±*k*, ±*l*), [(sinθ)/λ] = 0.54 Å⁻¹, 8179 independent (*R*_{int} = 0.000) and 5703 observed reflections [*I* ≥ 2σ(*I*)], 383 refined parameters, *R* = 0.159, *wR*² = 0.379, maximum residual electron density 0.88 (−0.55) e Å⁻³, poorly diffracting crystals. Analysis was performed to confirm the 'chemistry' of the formed complex. Only Ti, K, and the bridging oxygen atoms were refined with anisotropic thermal parameters, all other atoms were refined with isotropic thermal parameters. Severe, not refined disorder in some of the DMF molecules, hydrogens at N, O, and the solvate water molecules could not be located, other hydrogens were calculated and refined as riding atoms.

K₂[(3c)₂Ti(OCH₃)₂]: Yield: 66 mg (49%) as an orange solid: ¹H NMR ([D₄]methanol, 500 MHz, two major species **A** and **B**): δ = 9.91, 9.70 (2 × d, Σ = 1H, ratio: 0.25 (*J* = 9.2 Hz, **B**):1.0 (*J* = 9.5 Hz, **A**), 7.45–6.94 (m, 6H), 6.67–6.17 (m, 5H), 5.08–4.97 (m, 1H), 4.54, 4.15, 4.49, 4.27, 4.46, 4.17, 4.43, 4.01, 4.11 (4 × 2d, 1 × d, Σ = 2H, ratio: 0.25 (*J* = 14.8 Hz, **B**):0.04 (*J* = 15.2 Hz):1.0 (*J* = 14.1 Hz, **A**):0.04 (*J* = 14.5 Hz)), 3.37 (m, 1H, partly hidden under the signal of the solvent), 3.13 (m, 1H); ¹³C NMR ([D₄]methanol, 125.8 MHz): δ = 174.2 (C, **B**), 173.8 (C, **A**), 169.2 (C, **B**), 168.9 (C, **A**), 160.9 (C, **A**), 160.8 (C, **B**), 160.7 (C, **B**), 160.6 (C, **A**), 160.4 (C, **B**), 160.3 (C, **A**), 159.3 (C, **B**), 159.1 (C, **A**), 138.9 (C, **B**), 138.6 (C, **A**), 130.5 (CH, **A**, double intensity), 130.2 (CH, **B**, double intensity), 129.8 (CH, **A**, double intensity), 129.7 (CH, **B**, double intensity), 127.9 (CH, **A**), 127.8 (CH, **B**), 120.7 (CH, **A**), 120.3 (CH, **A**), 119.2 (CH, **A**), 119.2 (C, **A**), 119.0 (CH, **A**), 115.6 (C, **A**), 115.3 (CH, **A**), 114.9 (CH, **B**), 111.9 (CH, **B**), 111.5 (CH, **A**), 56.5 (CH, **B**), 56.2 (CH, **A**), 44.2 (CH₂, **B**), 43.8 (CH₂, **A**), 40.0 (CH₂, **B**), 39.9 (CH₂, **A**); IR (KBr): ν̄ = 3415, 3062, 1646, 1542, 1251, 742 cm⁻¹; UV/Vis (methanol): λ_{max} = 192, 205, 278, 393 nm; elemental analysis calcd (%) for C₄₈H₄₂K₂N₄O₁₄Ti₂·7 H₂O: C 48.08, H 4.71, N 4.67; found: C 47.85, H 4.71, N 4.53.

Na₂[(3c)₂Ti(OCH₃)₂]: Yield: 51 mg (73%) as a red solid: ¹H NMR ([D₄]methanol, 500 MHz): δ = 9.70 (d, 1H, *J* = 9.5 Hz), 7.60–6.96 (m, 6H), 6.65–6.18 (m, 5H), 5.13–4.99 (m, 1H), 4.56–4.39 (m, 1H), 4.31–3.99 (m, 1H), 3.37 (m, 1H, partly hidden under solvent signal), 3.15 (m, 1H); ¹³C NMR ([D₄]methanol, 125.8 MHz): δ = 173.8 (C), 169.0 (C), 168.9 (C), 160.9 (C), 160.6 (C), 160.3 (C), 159.1 (C), 138.6 (C), 130.4 (CH, double intensity), 129.8 (CH, double intensity), 127.9 (CH), 120.7 (CH), 120.3 (CH), 119.2 (CH), 119.0 (CH), 115.6, 115.6 (2 × C, ratio: 1 : 1), 115.3 (CH), 111.5 (CH), 56.3, 56.2 (2 × CH, ratio: 1 : 1), 43.8 (CH₂), 39.9 (CH₂); IR (KBr): ν̄ = 3396, 3061, 1641, 1536, 1252, 741 cm⁻¹; UV/Vis (methanol): λ_{max} = 192, 205, 277, 395 nm; negative-ion ESI MS (methanol): *m/z* 497 [(3c)₂Ti(OCH₃)₂]²⁻, 698 [(3c)₂TiNa₂]²⁻, 1017 [Na[(3c)₂Ti(OCH₃)₂]]⁻; elemental analysis calcd (%) for C₄₈H₄₂Na₂N₄O₁₄Ti₂·7 H₂O: C 49.41, H 4.84, N 4.80; found: C 49.31, H 5.14, N 4.72.

Li₂[(3c)₂Ti(OCH₃)₂]: Yield: 45 mg (64%) as a red solid: ¹H NMR ([D₄]methanol, 500 MHz): δ = 9.91, 9.70 (2 × d, Σ = 1H, ratio: 1.0 (*J* = 9.2 Hz):0.4 (*J* = 9.5 Hz)), 7.49–6.91 (m, 6H), 6.62–6.12 (m, 5H), 5.03 (m, 1H), 4.48 (m, 1H), 4.28, 4.27, 4.25, 4.17, 4.15, 4.09, 4.01 (7 × d, Σ = 1H, ratio: 0.1 (*J* = 14.8 Hz): 0.4 (*J* = 14.8 Hz):0.1 (*J* = 14.8 Hz)): 1.0 (*J* = 14.5 Hz, **A**): 0.5 (*J* = 14.8 Hz, **B**):0.4 (*J* = 14.8 Hz):0.1 (*J* = 13.4 Hz)), 3.38 (m, 1H, partly hidden under solvent signal), 3.10 (m, 1H); ¹³C NMR ([D₄]methanol, 125.8 MHz): δ = 174.2 (C, **B**), 173.8 (C, **A**), 169.2 (C, **B**), 168.9 (C, **A**), 160.9 (C, **A**), 160.8 (C, **B**), 160.7 (C, **B**), 160.6 (C, **A**), 160.4 (C, **B**), 160.3 (C, **A**), 159.3 (C, **B**), 159.1 (C, **A**), 138.9 (C, **B**), 138.6 (C, **A**), 130.5 (CH, **A**, double intensity), 130.2 (CH, **B**, double intensity), 129.8 (CH, **A**, double intensity), 129.7 (CH, **B**, double intensity), 127.9 (CH, **A**), 127.8 (CH, **B**), 120.7 (CH, **A**), 120.3 (CH, **A**), 119.2 (CH, **A**), 119.1 (CH, **A**), 119.0 (CH, **A**), 115.6 (C, **A**), 115.3 (CH, **A**), 114.9 (CH, **B**), 111.9 (CH, **B**), 111.5 (CH, **A**), 56.5 (CH, **B**), 56.2 (CH, **A**), 44.3 (CH₂, **B**), 43.8 (CH₂, **A**), 40.0 (CH₂, **B**), 39.9 (CH₂, **A**); IR (KBr): ν̄ = 3370, 3062, 1636, 1518, 1258, 740 cm⁻¹; UV/Vis (methanol): λ_{max} = 192, 206, 276, 380 nm; negative-ion ESI MS (methanol): *m/z* 497 [(3c)₂Ti(OCH₃)₂]²⁻, 1001 [Li[(3c)₂Ti(OCH₃)₂]]⁻; elemental analysis calcd (%) for C₄₈H₄₂Li₂N₄O₁₄Ti₂·4 H₂O: C 53.35, H 4.66, N 5.18; found: C 53.52, H 4.92, N 5.02.

K₂[(3d)₂Ti(OCH₃)₂]: Yield: 30 mg (47%) as an orange solid: ¹H NMR ([D₄]methanol, 500 MHz): δ = 9.83, 9.68 (2 × d, Σ = 1H, ratio: 0.3 (*J* = 9.2 Hz): 1.0 (*J* = 8.8 Hz)), 7.29, 7.24, 7.22, 7.19 (4 × dd, Σ = 1H, ratio: 0.02 (*J* = 8.1, 1.4 Hz): 0.1 (*J* = 8.1, 1.7 Hz): 1.0 (*J* = 8.1, 1.4 Hz): 0.3 (*J* = 8.1, 1.4 Hz)), 6.62–6.23 (m, 5H), 4.76, 4.70 (2 × m, Σ = 1H), 4.56, 4.41, 4.16, 4.02 (4 × m, Σ = 2H), 1.98 (m, 1H), 1.92–1.75 (m, 2H), 1.06, 1.02, 0.92, 0.88, 0.81 (5 × m, Σ = 6H); IR (KBr): ν̄ = 3403, 3062, 1644, 1547, 1251, 740, 634 cm⁻¹; UV/Vis (methanol): λ_{max} = 205, 278, 382, 398 nm; negative-ion ESI-MS (methanol): *m/z* 463 [(3d)₂Ti(OCH₃)₂]²⁻, 664 [K₂[(3d)₂Ti]²⁻] (traces), 928 [H[(3d)₂Ti(OCH₃)₂]]⁻, 966 [K[(3d)₂Ti(OCH₃)₂]]⁻; elemental analysis calcd (%) for C₄₂H₄₆N₄O₁₄Ti₂·2.5 H₂O: C 48.05, H 4.90, N 5.34; found: C 48.03, H 5.30, N 5.34.

X-ray quality crystals of K₂[(3d)₂Ti(OH)₂] were obtained from wet DMF/diethyl ether. X-ray crystal structure analysis of K₂[(3d)₂Ti(OH)₂]: formula C₄₀H₄₂N₄O₁₄K₂Ti₂·6 C₃H₇NO, *M_r* = 1415.35, red crystal 0.65 × 0.20 × 0.05 mm, *a* = 12.946(1), *b* = 20.246(1), *c* = 27.034(1) Å, *V* = 7085.7(7) Å³, ρ_{calcd} = 1.327 g cm⁻³, μ = 4.17 cm⁻¹, no absorption correction (0.773 ≤ *T* ≤ 0.980), *Z* = 4, orthorhombic, space group *P*2₁2₁2₁ (no. 19), λ = 0.71073 Å, *T* = 198 K, ω and φ scans, 9240 reflections collected (±*h*, ±*k*, ±*l*), [(sinθ)/λ] = 0.54 Å⁻¹, 9240 independent (*R*_{int} = 0.000) and 7082 observed reflections (*I* > 2σ(*I*)), 797 refined parameters, *R* = 0.076, *wR*² = 0.187, maximum residual electron density 0.62 (−0.42) e Å⁻³, two of the six independent DMF molecules (O91–C95, O121–C125) are heavily disordered, refined with isotropic thermal displacement parameters, hydrogens at N and O found from difference Fourier calculations, refined with constraints (SADI), other hydrogen atoms were calculated and refined as riding atoms.

Na₂[(3d)₂Ti(OCH₃)₂]: Yield: 44 mg (70%) of a red solid: ¹H NMR ([D₄]methanol, 500 MHz): δ = 9.84, 9.68 (2 × d, Σ = 1H, ratio: 0.4 (*J* = 8.8 Hz): 1.0 (*J* = 9.2 Hz)), 7.72, 7.63 (2 × d, Σ = 1H, ratio: 0.8 (*J* = 4.9 Hz): 1.0 (*J* = 5.7 Hz)), 7.30, 7.25, 7.22, 7.19 (4 × dd, Σ = 1H, ratio: 0.04 (*J* = 7.9, 1.6 Hz): 0.2 (*J* = 8.1, 1.4 Hz): 1.0 (*J* = 8.0, 1.6 Hz): 0.4 (*J* = 8.0, 1.6 Hz)), 6.62–6.24 (m, 5H), 4.78, 4.70 (2 × m, Σ = 1H), 4.55, 4.41, 4.16, 4.02 (4 × m, Σ = 2H), 1.98 (m, 1H), 1.92–1.75 (m, 2H), 1.06, 1.02, 0.92, 0.80 (4 × m, Σ = 6H); ¹³C NMR ([D₄]methanol, 125.8 MHz): δ = 175.7 (C), 175.7 (C), 175.4 (C), 174.9 (C), 169.3 (C), 169.2 (C), 169.0 (C), 168.9 (C), 161.1 (C), 160.7 (C), 160.6 (C), 160.4 (C), 160.3 (C), 160.2 (C), 159.0 (C), 159.0 (C), 121.1 (CH), 120.7 (CH), 120.7 (CH), 120.5 (CH), 120.2 (CH), 119.9 (CH), 119.4 (CH), 119.2 (CH), 119.1 (CH), 118.8 (CH), 115.9 (C), 115.8 (C), 115.6 (C), 115.5 (C), 115.2 (CH), 114.9 (CH), 112.3 (CH), 111.8 (CH), 111.5 (CH), 53.6 (CH), 53.5 (CH), 53.4 (CH), 53.2 (CH), 44.4, 44.3, 44.1, 43.9 (4 × CH₂, ratio: 0.2:0.4:1.0:0.1), 43.4 (CH₂), 43.4 (CH₂), 43.2 (CH₂), 26.2, 26.1, 25.9, 25.7 (4 × CH, ratio: 1.0:0.4:0.1:0.2), 23.8 (CH₃), 22.1, 21.8, 21.6, 21.5 (4 × CH₃, ratio: 0.1:0.04:1.0:0.4); IR (KBr): ν̄ = 3393, 3063, 1642, 1546, 1252, 741, 635 cm⁻¹; UV/Vis (methanol): λ_{max} = 205, 278, 382, 395 nm; negative-ion ESI-MS (methanol): *m/z*: 463 [(3d)₂Ti(OCH₃)₂]²⁻, 647 [Na₂[(3d)₂Ti]²⁻] (traces), 950 [Na[(3d)₂Ti(OCH₃)₂]]⁻; elemental analysis calcd (%) for C₄₂H₄₆Na₂O₁₄Ti₂·3 H₂O: C 49.14, H 5.11, N 5.46; found: C 48.59, H 5.46, N 5.37.

Li₂[(3d)₂Ti(OCH₃)₂]: Yield: 44 mg (72%) of a red solid: ¹H NMR ([D₄]methanol, 500 MHz): δ = 9.84, 9.68 (2 × d, Σ = 1H, ratio: 0.3 (*J* = 8.8 Hz): 1.0 (*J* = 8.8 Hz)), 7.71, 7.62 (2 × d, Σ = 1H, ratio: 0.3 (*J* = 4.2 Hz): 1.0 (*J* = 6.0 Hz)), 7.29, 7.25, 7.22, 7.18 (4 × dd, Σ = 1H, ratio: 0.02 (*J* = 8.1, 1.8 Hz): 0.1 (*J* = 8.1, 1.4 Hz): 1.0 (*J* = 7.8, 1.4 Hz): 0.3 (*J* = 7.8, 1.4 Hz)), 6.62–6.22 (m, 5H), 4.79, 4.70 (2 × m, Σ = 1H), 4.55, 4.41, 4.16, 4.01 (4 × m, Σ = 2H), 1.99 (m, 1H), 1.92–1.75 (m, 2H), 1.06, 1.02, 0.92, 0.81 (4 × m, Σ = 6H); ¹³C NMR ([D₄]methanol, 125.8 MHz, **A** and **B** indicate signals of the two major species): δ = 175.6 (C, **B**), 175.3 (C, **A**), 169.2 (C, **B**), 168.9 (C, **A**), 161.1 (C, **A**), 160.7 (C, **B**), 160.6 (C, **B**), 160.4 (C, **B**), 160.3 (C, **A**), 160.2 (C, **A**), 159.1 (C, **A**), 159.0 (C, **B**), 120.7 (CH, **A**), 120.5 (CH, **A**), 119.9 (CH), 119.4 (CH, **A**), 119.2 (C, **A**), 119.1 (CH, **A**), 118.8 (CH), 118.6 (CH), 115.8 (C, **A**), 115.5 (C, **B**), 115.2 (CH, **A**), 114.9 (CH, **B**), 111.8 (CH, **B**), 111.5 (CH, **A**), 53.4 (CH, **B**), 53.4 (CH, **A**), 44.3 (CH₂, **B**), 44.1 (CH₂, **A**), 43.4 (CH₂, **A**), 43.2 (CH₂, **B**), 26.2 (CH, **A**), 26.1 (CH, **B**), 23.8 (CH₃, **A**), 23.7 (CH₃, **B**), 21.6 (CH₃, **A**), 21.5 (CH₃, **B**); IR (KBr): ν̄ = 3403, 2958, 1647, 1559, 1252, 741, 636 cm⁻¹; UV/Vis (methanol): λ_{max} = 205, 277, 398 nm; negative-ion ESI-MS (methanol): *m/z*: 463 [(3d)₂Ti(OCH₃)₂]²⁻, 934 [Li[(3d)₂Ti(OCH₃)₂]]⁻; elemental analysis calcd (%) for C₄₂H₄₆N₄Li₂O₁₄Ti₂·4.5 H₂O: C 49.38, H 5.43; found: C 49.67, H 5.92, N 5.38.

K₂[(3e)₂Ti(OCH₃)₂]: Yield: 30 mg (46%) as a red solid: ¹H NMR ([D₄]methanol, 500 MHz): δ = 9.71, 9.56, 9.48, 9.38 (4 × d, Σ = 1H, ratio:

0.6 ($J = 9.5$ Hz): 0.15 ($J = 9.5$ Hz): 1.0 ($J = 10.3$ Hz): 0.1 ($J = 9.5$ Hz)), 7.31, 7.27, 7.25, 7.22 ($4 \times$ dd, $\Sigma = 1$ H, ratio: 0.1 ($J = 1.4$, 8.1 Hz): 0.4 ($J = 1.4$, 8.1 Hz): 1.0 ($J = 1.6$, 8.0 Hz): 0.6 ($J = 1.6$, 7.9 Hz)), 6.63–6.36 (m, 4H), 6.29–6.20 (m, 1H), 4.78, 4.69, 4.62 (3 m, $\Sigma = 1$ H), 4.46, 4.41 ($2 \times$ d, $\Sigma = 1$ H, ratio: 0.6 ($J = 14.3$ Hz): 1.0 ($J = 14.3$ Hz)), 4.18, 4.02 (d and dd, $\Sigma = 1$ H, ratio: 1.0 ($J = 15.0$ Hz): 0.6 ($J = 3.2$, 13.4 Hz)): 2.56, 2.47, 2.35 ($3 \times$ m, $\Sigma = 1$ H, ratio: 1.0:0.6:0.4), 1.22, 1.19, 0.99 ($3 \times$ d, $\Sigma = 3$ H, ratio: 0.6 ($J = 7.1$ Hz): 1.0 ($J = 7.1$ Hz): 0.4 ($J = 6.7$ Hz)), 1.13, 1.11, 0.70 ($4 \times$ d, $\Sigma = 3$ H, ratio: 0.6 ($J = 7.1$ Hz): 1.0 ($J = 6.7$ Hz): 0.4 ($J = 7.1$ Hz): 0.1 ($J = 7.1$ Hz)); ^{13}C NMR ($[\text{D}_2]$ methanol, 125.8 MHz): $\delta = 174.4$ (C), 174.2 (C), 174.1 (C), 173.9 (C), 169.7 (C), 169.6 (C), 169.5 (C), 169.3 (C), 169.3 (C), 160.8 (C), 160.5 (C), 160.5 (C), 160.4 (C), 160.4 (C), 160.0 (C), 159.8 (C), 159.1 (C), 159.0 (C), 121.3 (C), 121.0 (CH), 120.7 (CH), 120.7 (CH), 120.5 (CH), 119.9 (CH), 119.4 (CH), 119.3 (C), 119.2 (C), 119.1 (CH), 118.8 (CH), 116.2 (C), 116.0 (CH), 116.0 (CH), 115.7 (CH), 115.7 (C), 115.5 (CH), 115.4 (CH), 115.0 (CH), 112.3 (CH), 111.9 (CH), 111.6 (CH), 60.4 (CH), 60.3 (CH), 59.8 (CH), 59.7 (CH), 59.4 (CH), 59.3 (CH), 44.0 (CH₂), 43.5 (CH₂), 31.9, 31.8, 31.5 ($3 \times$ CH, ratio: 0.6:1.0:0.4), 20.2, 20.1, 20.1, 20.0 ($4 \times$ CH₃, ratio: 0.6:1.0:0.1:0.4), 18.8, 18.3, 16.7, 16.6 ($4 \times$ CH₃, ratio: 0.6:1.0:0.4:0.1); IR (KBr): $\tilde{\nu} = 3403$, 3066, 1644, 1547, 1251, 742 cm^{-1} ; UV/Vis (methanol): $\lambda_{\text{max}} = 206$, 278, 405 nm; negative-ion ESI-MS (methanol): m/z : 449 ($[(\mathbf{3e})_2\text{Ti}_2(\text{OCH}_3)_2]^-$), 938 ($[\text{K}[(\mathbf{3e})_2\text{Ti}_2(\text{OCH}_3)_2]^-]$); elemental analysis calcd (%) for C₄₀H₄₂N₄K₂O₁₄Ti₂·4H₂O: C 45.82, H 4.81, N 5.34; found: C 46.01, H 5.03, N 5.32.

Na₂[(3e**)₂Ti₂(OCH₃)₂]**: Yield: 47 mg (74%) of a red solid: ^1H NMR ($[\text{D}_2]$ methanol, 500 MHz): $\delta = 9.71$, 9.56, 9.48, 9.38 ($4 \times$ d, $\Sigma = 1$ H, ratio: 0.5 ($J = 9.5$ Hz): 0.1 ($J = 9.5$ Hz): 1.0 ($J = 9.9$ Hz): 0.2 ($J = 9.5$ Hz)), 7.30, 7.27, 7.25, 7.21 ($4 \times$ dd, $\Sigma = 1$ H, ratio: 0.1 ($J = 1.8$, 8.1 Hz): 0.2 ($J = 1.4$, 8.1 Hz): 1.0 ($J = 1.4$, 8.1 Hz): 0.5 ($J = 1.8$, 7.8 Hz)), 6.69–6.35 (m, 4H), 6.30–6.19 (m, 1H), 4.78, 4.70, 4.61 ($3 \times$ m, $\Sigma = 1$ H), 4.45, 4.40, 4.36 ($3 \times$ d, $\Sigma = 1$ H, ratio: 0.5 ($J = 13.1$ Hz): 1.0 ($J = 14.1$ Hz): 0.2 ($J = 13.4$ Hz)), 4.18, 4.02 ($2 \times$ m, $\Sigma = 1$ H), 2.51, 2.47, 2.34 ($3 \times$ m, $\Sigma = 1$ H, ratio: 1.0:0.5:0.2), 1.22, 1.19, 0.99 ($3 \times$ d, $\Sigma = 3$ H, ratio: 0.5 ($J = 6.7$ Hz): 1.0 ($J = 6.7$ Hz): 0.2 ($J = 7.1$ Hz)), 1.12, 1.11, 0.67 ($3 \times$ d, $1 \times$ m, $\Sigma = 3$ H, ratio: 0.5 ($J = 6.7$ Hz): 1.0 ($J = 7.1$ Hz): 0.2); IR (KBr): $\tilde{\nu} = 3403$, 3066, 1649, 1547, 1251, 741 cm^{-1} ; UV/Vis (methanol): $\lambda_{\text{max}} = 205$, 278, 404 nm; negative-ion ESI-MS (methanol): m/z : 449 ($[(\mathbf{3e})_2\text{Ti}_2(\text{OCH}_3)_2]^-$), 626 ($[\text{Na}_2[(\mathbf{3e})_2\text{Ti}_2]^-]$ (traces), 900 ($[\text{H}[(\mathbf{3e})_2\text{Ti}_2(\text{OCH}_3)_2]^-]$), 922 ($[\text{Na}[(\mathbf{3e})_2\text{Ti}_2(\text{OCH}_3)_2]^-]$); elemental analysis calcd (%) for C₄₀H₄₂N₄Na₂O₁₄Ti₂·4H₂O: C 47.26, H 4.96, N 5.51; found: C 47.29, H 5.38, N 5.72.

One X-ray quality crystal of Na₂[(**3e**)(**3e'**)Ti₂(OCH₃)₂] was obtained from wet DMF/diethyl ether. X-ray crystal structure analysis of Na₂[(**3e**)(**3e'**)Ti₂(OCH₃)₂]: formula C₄₀H₄₂N₄O₁₄Na₂Ti₂·4C₃H₇NO·C₄H₁₀O, $M_r = 1311.06$, red crystal $0.25 \times 0.20 \times 0.10$ mm, $a = 9.088(1)$, $b = 13.638(1)$, $c = 14.696(1)$ Å, $\alpha = 112.01(1)$, $\beta = 96.52(1)$, $\gamma = 100.59(1)^\circ$, $V = 1626.3(2)$ Å³, $\rho_{\text{calcd}} = 1.339$ g cm⁻³, $\mu = 3.33$ cm⁻¹, empirical absorption correction by SORTAV ($0.921 \leq T \leq 0.967$), $Z = 1$, triclinic, space group $P\bar{1}$ (no. 2), $\lambda = 0.71073$ Å, $T = 198$ K, ω and φ scans, 17033 reflections collected ($\pm h$, $\pm k$, $\pm l$), $[\text{sin}\theta/\lambda] = 0.66$ Å⁻¹, 7615 independent ($R_{\text{int}} = 0.043$) and 5403 observed reflections ($I \geq 2\sigma(I)$), 457 refined parameters, $R = 0.060$, $wR^2 = 0.136$, maximum residual electron density 0.56 (–0.42) e Å⁻³. One of the two independent DMF molecules is disordered, and was refined with geometrical split positions in a ratio of 0.70:0.30(1); the ether molecules is also disordered in a ratio of 0.70:0.30(1). Atoms of this molecule were refined with common isotropic thermal displacement parameter, hydrogen atoms calculated and refined as riding atoms.

Li₂[(3e**)₂Ti₂(OCH₃)₂]**: Yield: 54 mg (88%) as a red solid: ^1H NMR ($[\text{D}_2]$ methanol, 500 MHz): $\delta = 9.71$, 9.56, 9.48, 9.38 ($4 \times$ d, $\Sigma = 1$ H, ratio: 0.6 ($J = 9.5$ Hz): 0.05 ($J = 10.2$ Hz): 1.0 ($J = 9.9$ Hz): 0.1 ($J = 9.2$ Hz)), 7.31, 7.27, 7.25, 7.21 ($4 \times$ dd, $\Sigma = 1$ H, ratio: 0.1 ($J = 1.4$, 8.1 Hz): 0.3 ($J = 1.4$, 8.1 Hz): 1.0 ($J = 1.4$, 8.1 Hz): 0.6 ($J = 1.8$, 8.1 Hz)), 6.63–6.36 (m, 4H), 6.30–6.14 (m, 1H), 4.78, 4.69, 4.62 (3 m, $\Sigma = 1$ H), 4.45, 4.40, 4.35, 4.26 ($4 \times$ m, $\Sigma = 1$ H), 4.18, 4.10, 4.02 ($4 \times$ m, $\Sigma = 1$ H), 2.52, 2.47, 2.34 ($3 \times$ m, $\Sigma = 1$ H, ratio: 1.0:0.6:0.3), 1.24, 1.22, 1.00 ($4 \times$ d, $\Sigma = 3$ H, ratio: 0.1 ($J = 6.7$ Hz): 0.6 ($J = 6.7$ Hz): 1.0 ($J = 6.7$ Hz): 0.3 ($J = 6.7$ Hz)), 1.12, 1.11, 1.00 ($3 \times$ d, $\Sigma = 3$ H, ratio: 0.6 ($J = 6.4$ Hz): 1.0 ($J = 6.7$ Hz): 0.3 ($J = 7.1$ Hz)); ^{13}C NMR ($[\text{D}_2]$ methanol, 125.8 MHz, **A** corresponds to the dominating isomer): $\delta = 174.4$ (C), 174.2 (C), 173.9 (C, **A**), 169.6 (C), 169.5 (C), 169.3 (C, **A**), 160.8 (C, **A**), 160.5 (C), 160.4 (C, **A**), 160.4 (C), 160.1 (C, **A**), 159.8 (C), 159.1 (C, **A**), 159.0 (C), 121.0 (CH, **A**), 120.7 (CH), 120.7 (CH), 120.5 (CH, **A**), 120.0 (CH), 119.4 (CH, **A**), 119.3 (C, **A**), 119.2 (C), 119.1 (CH, **A**), 118.8 (CH),

116.2 (C), 115.9 (C, **A**), 115.7 (C), 115.5 (CH, **A**), 115.4 (CH), 115.0 (CH), 112.3 (CH), 111.9 (CH), 111.6 (CH, **A**), 60.2 (CH), 59.7 (CH, **A**), 59.2 (CH), 44.0 (CH₂), 43.5 (CH₂, **A**), 31.9 (CH), 31.8 (CH, **A**), 31.6 (CH), 20.2 (CH₃), 20.1 (CH₃, **A**), 20.0 (CH₃), 18.8 (CH₃), 18.2 (CH₃, **A**), 16.7 (CH₃); IR (KBr): $\tilde{\nu} = 3403$, 2964, 1642, 1528, 1252, 741 cm^{-1} ; UV/Vis (methanol): $\lambda_{\text{max}} = 205$, 277, 399 nm; negative-ion ESI-MS (methanol): m/z : 449 ($[(\mathbf{3e})_2\text{Ti}_2(\text{OCH}_3)_2]^-$), 900 ($[\text{H}[(\mathbf{3e})_2\text{Ti}_2(\text{OCH}_3)_2]^-]$), 906 ($[\text{Li}[(\mathbf{3e})_2\text{Ti}_2(\text{OCH}_3)_2]^-]$); elemental analysis calcd (%) for C₄₀H₄₂N₄Li₂O₁₄Ti₂·6H₂O: C 47.08, H 5.33, N 5.49; found: C 47.31, H 5.63, N 5.28.

Acknowledgements

This work was supported by the Deutsche Forschungsgemeinschaft and the Fonds der Chemischen Industrie. We thank Prof. Dr. M. Kappes and the Nanotechnology Institute, Forschungszentrum Karlsruhe for facilitating the ESI-MS measurements.

- [1] a) S. J. Lippard, J. M. Berg, *Principles in Bioinorganic Chemistry*, University Science Books, Mill Valley, **1994**; b) A. L. Feig, S. J. Lippard, *Chem. Rev.* **1994**, 94, 759; c) N. Sträter, W. N. Lipscomb, T. Klubunde, B. Krebs, *Angew. Chem.* **1996**, 108, 2158; *Angew. Chem. Int. Ed. Engl.* **1996**, 35, 2024.
- [2] E. C. Constable, *Tetrahedron* **1992**, 48, 10013.
- [3] C. Piguet, G. Bernardinelli, G. Hopfgartner, *Chem. Rev.* **1997**, 97, 2005.
- [4] M. Albrecht, *Chem. Soc. Rev.* **1998**, 27, 281.
- [5] a) W. B. Tolman, *Acc. Chem. Res.* **1997**, 30, 227; b) K. Wieghardt, *Angew. Chem.* **1989**, 1179; *Angew. Chem. Int. Ed. Engl.* **1989**, 28, 1153.
- [6] E. J. Enemark, T. D. P. Stack, *Inorg. Chem.* **1996**, 35, 2719.
- [7] M. Albrecht, H. Röttele, P. Burger, *Chem. Eur. J.* **1996**, 2, 1264.
- [8] M. Albrecht, M. Napp, M. Schneider, *Synthesis* **2001**, 468.
- [9] C. J. Carrano, K. N. Raymond, *J. Am. Chem. Soc.* **1978**, 100, 5371.
- [10] For selected examples of the coordination chemistry of dicatechol ligands, see: a) E. J. Enemark, T. D. P. Stack, *Angew. Chem.* **1995**, 107, 1082; *Angew. Chem. Int. Ed. Engl.* **1995**, 34, 996; b) B. Kersting, M. Meyer, R. E. Powers, K. N. Raymond, *J. Am. Chem. Soc.* **1996**, 118, 7221; c) A.-K. Duhme, Z. Dauter, R. C. Hider, S. Pohl, *Inorg. Chem.* **1996**, 35, 3059; d) M. Albrecht, S. Kotila, *Angew. Chem.* **1995**, 107, 2285; *Angew. Chem. Int. Ed. Engl.* **1995**, 34, 2134.
- [11] M. Albrecht, M. Napp, M. Schneider, P. Weis, R. Fröhlich, *Chem. Commun.* **2001**, 409.
- [12] a) E. J. Corey, C. L. Cywin, M. C. Noe, *Tetrahedron Lett.* **1994**, 35, 69; b) A. Von Zelewsky, O. Mamula, *J. Chem. Soc. Dalton Trans.* **2000**, 219.
- [13] M. Albrecht, *Synlett* **1996**, 565.
- [14] M. Albrecht, M. Napp, M. Schneider, *Synthesis* **2001**, 468.
- [15] a) E. C. Constable, M. Neuburger, D. R. Smith, M. Zehnder, *Chem. Commun.* **1996**, 1917; b) C. Piguet, J.-C. G. Bünzli, G. Bernardinelli, G. Hopfgartner, S. Petoud, O. Schaad, *J. Am. Chem. Soc.* **1996**, 118, 6681; c) M. J. Hannon, S. Bunce, A. I. Clarke, N. W. Alcock, *Angew. Chem.* **1999**, 111, 1353; *Angew. Chem. Int. Ed. Engl.* **1999**, 38, 1277; d) M. Albrecht, R. Fröhlich, *J. Am. Chem. Soc.* **1997**, 119, 1656.
- [16] M. Albrecht, *Chem. Eur. J.* **2000**, 6, 3485.
- [17] a) K. Severin, W. Beck, G. Trojandt, K. Polborn, W. Steglich, *Angew. Chem.* **1995**, 107, 1570; *Angew. Chem. Int. Ed. Engl.* **1995**, 34, 1449; b) H. Stoeckli-Evans, *Helv. Chim. Acta* **1975**, 58, 373; c) T. V. Lubben, P. T. Wolczanski, *J. Am. Chem. Soc.* **1987**, 109, 424; d) W. Scharf, D. Neugebauer, U. Schubert, H. Schmidbaur, *Angew. Chem.* **1978**, 90, 628; *Angew. Chem. Int. Ed. Engl.* **1978**, 17, 601.
- [18] W. Zarges, J. Hall, J.-M. Lehn, C. Bolm, *Helv. Chim. Acta* **1991**, 74, 1843.
- [19] M. Albrecht, S. Kotila, *Angew. Chem.* **1996**, 108, 1299; *Angew. Chem. Int. Ed. Engl.* **1996**, 35, 1208.
- [20] M. Bodanszky, A. Bodanszky, *The Practice of Peptide Synthesis*, Springer, Berlin, **1984**.
- [21] a) M. Albrecht, S. J. Franklin, K. N. Raymond, *Inorg. Chem.* **1994**, 33, 5785; b) T. B. Karpishin, T. D. P. Stack, K. N. Raymond, *J. Am. Chem. Soc.* **1993**, 115, 6115.
- [22] G. N. Ramachandran, V. Sasiskharan, *Adv. Protein Chem.* **1968**, 23, 283.

- [23] T. E. Creighton, *Proteins, Structures and Molecular Properties*, W. H. Freeman, New York, **1984**.
- [24] A. Fersht, *Structure and Mechanism in Protein Science*, W. H. Freeman, New York, **1998**.
- [25] Z. Otwinowski, W. Minor, *Methods in Enzymology* **1997**, 276, 307.
- [26] a) R. H. A. C. Blessing, *Acta Cryst.* **1995**, A51, 33; b) R. H. A. C. Blessing, *J. Appl. Cryst.* **1997**, 30, 421.
- [27] G. M. Sheldrick, *Acta Crystallogr. Sect. A* **1990**, 46, 467.
- [28] E. Keller, Schakal 97, Universität Freiburg **1997**.

Received: March 29, 2001 [F3163]